Robotic Autonomous Field Gamma Radiation Measurement for Environmental Protection

LUDEK ZALUD[1], TOMAS JILEK[1], PETRA KOCMANOVA[1,2]
[1]LTR s.r.o.
U Vodarny 2032/2a, Brno
Czech Republic
zalud@orpheus-project.cz, http://www.orpheus-project.cz
[2]CEITEC
Brno University of Technology
Technicka 12, Brno
Czech Republic
petra.kocmanova@ceitec.vutbr.cz

Abstract: - Two gamma-radiation distribution field measurement experiments are described in the paper. Because of principally dangerous nature of gamma-radiation, the idea was to extensively use robotic systems and automation to minimize human exposure to radiation. The experiment setup as well as Orpheus robotic system are described. Algorithm to autonomously navigate the robot based on RTK GNSS in predefined area is presented. The algorithm was exclusively developed for Orpheus robot, considering its tank-like drive configuration.

Key-Words: - robot, gamma-radiation, measurement, automatic navigation, precise satellite self-localization, telepresence, augmented reality, visual control, robotic reconnaissance

1 Introduction

Reconnaissance mobile robotics gains importance during the last years. There are many missions in today's society that may require expendable robots to perform exploration in inaccessible or dangerous environments instead of indispensable people, e.g. CBRNE (Chemical, biological, radio-logical, nuclear, explosive), counter-terrorist fight, US&R (Urban Search and Rescue), etc.

One of promising applications is outdoor radiation distribution measurement. The high demand for exclusion of people from direct measurement is obvious – radiation is not directly observable by people, but it may be extremely dangerous for our life. The radiation impact to our bodies is somewhat cumulative, so even for experiments and/or practical missions with relatively low radiation levels it is reasonable to minimize the human exposition. The situation is similar or in many aspects identical for chemical and/or biological contamination measurements, so mostly the same equipment and similar algorithms may be used.

It is typical to construct one combined vehicles or devices indicated as CBRN. See Figure 1 for example of relatively universal CBRN robot developed by our team. Orpheus-AC2 robot is extremely rugged machine, but its main drawback is that it is solely teleoperated robot. So the operator has to be in the reach of the robot-to-vehicle communication device and has to control the robot in real-time during the whole mission. This approach is very profitable for several missions, like primary contamination measurement in potentially heavily contaminated areas with other possible risks (explosives, antagonist opposition, etc.), but has its limits in other missions, where bigger area of interest with typically lower radiation levels has to be examined.

The aim of our team is now to develop autonomous exploration/measurement in predefined area. Since this task is, in general, extremely ambitious, we decided to restrict it to well defined, unstructured outdoor environments, like meadows, agricultural fields, etc. The idea is that the operator defines four outlaying points in the field, the separation among measurements is defined, and the robot automatically calculates the path and makes the measurement fully autonomously. For robot precise self-localization, RTK-GNSS is used. The same data are used also for logging of position and radiation data with corresponding time-stamp during measurement.

ISBN: 978-1-61804-356-6

Fig. 1 Orpheus-AC2 military robot for CBRN operator-controlled reconnaissance.

2 System Description

The aim of this chapter is to describe the system that was used during the two experiments described in the next chapter.

Our team is highly involved in development of extremely durable robots for contaminated areas. We have developed three different mid-size robots (approx. 50 kg) for both military and non-military missions in potentially contaminated areas. They are called Orpheus-AC-P, Orpheus-AC, and Orpheus-AC2 [7], [11]. These robots passed through 18 MIL-STD tests, including their ability to withstand contamination and decontamination. Although they might seem ideal for such an application, for several reasons we were not able to use these robots during the hereinafter described experiments. We had to use non-military robot Orpheus-X3 that is not prepared for contamination, but is very flexible when mechanical and electronics modifications have to be done, as in our case.

2.1 Orpheus-X3

Orpheus-X3 [8], [9], [10] is non-military robot belonging to the same generation as Orpheus-AC2.

The main parameters of Orpheus-X3 robot are in Table 1.

Table 1. Orpheus-X3 parameters

Parameter	**Value**
Dimensions (lxwxh)	950x590x415 mm
Weight	51 kg
Operation time	120 mins
Drive type	Differential
Maximum speed	15 km/h

For the first experiment, the robot was covered by plastic bags to be protected against possible contamination by the radioactive dust. The robot was carefully scanned for radiation after the experiment.

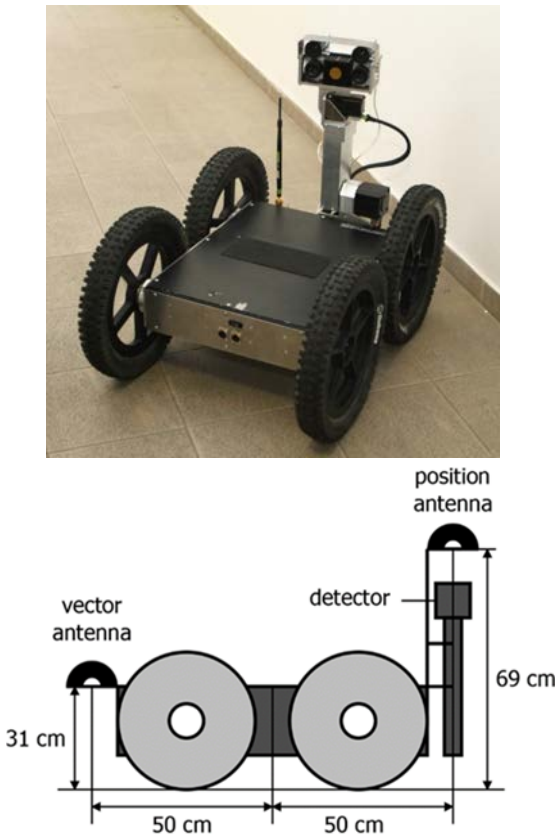

Fig. 2 Orpheus-X3 photo before modification (left), sensor and antennas placement (right).

The robot construction was modified for the experiments. The sensory head was not used, so it was deactivated. Trimble embedded RTK GNSS with two antennas was used for precise navigation and measurement. Custom made scintillation gamma-radiation probe with precise time derived from on-device GPS receiver, connected to data logger was used to measure radiation intensity.

ISBN: 978-1-61804-356-6

Since these devices are relatively large and must be exactly and rigidly placed on the robot, we developed custom metal frame. The main advantage is placement of the main antenna above the radiation sensor – that means the position data for radiation data-logging do not need to be recalculated – height is not considered, since it is supposed to be equal during the experiment (see Figure 2).

2.2 Trimble RTK GNSS

Two Trimble BX982 RTK GNSS receivers were used for precise position and orientation measurement of Orpheus-X3 robot during the experiments. One of them was used as stationery base-station, the other one was used onboard the robot in rover configuration.

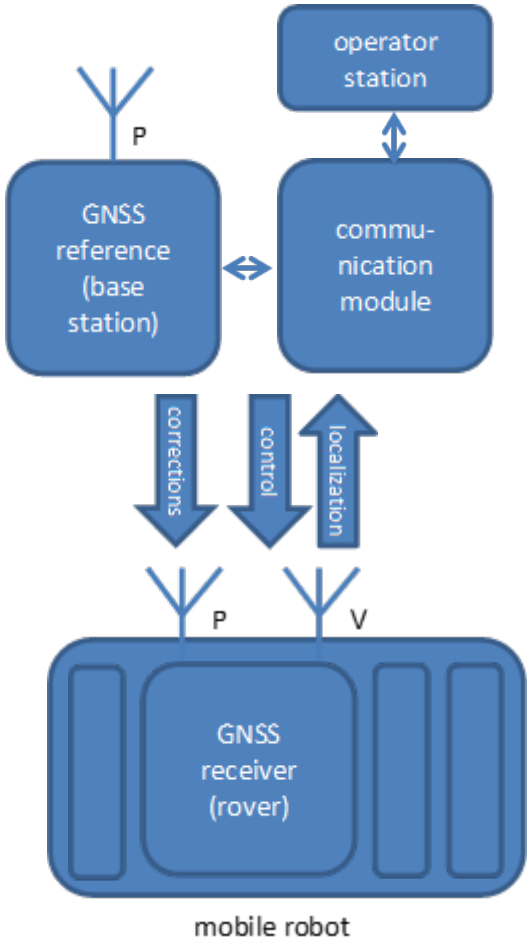

Fig. 3 GNSS configuration. P - position antenna, V - vector antenna

Table 2. Trimble BX982 embedded GNSS dual-antenna receiver main parameters [1]

Parameter	**Value**
Number of channels	220
GNSS supported	GPS, GLONASS
RTK	supported
Dual input for azimuth calculation	supported
Power	9-28 V DC, max. 5 W
Weight	1.6 kg
Size	264 mm x 140 mm x 55 mm
Operating temperature	-40 °C - +70 °C

The GNSS measurement configuration is on Figure 3. Although we used two identical modules, their configuration was different. The module named as Base station contained only one antenna input, and the main module used is RTK BASE. The other embedded module on the other hand had the dual-input enabled, as well as RTK ROVER. The calculation frequency on both modules was 50 Hz.

Fig. 4 Orpheus robot during the First experiment. Vital parts were covered by plastic bags as radiation dust protection.

ISBN: 978-1-61804-356-6

The robot GNSS was used also for azimuth measurement in double-antenna configuration. As it is visible from Figure 4, the antennas were not placed in the same height. The reason was purely practical – we decided to place the main antenna above the radiation detector, so the latitude and longitude coming from it corresponds approximately to the ones of the sensor. Inaccuracy caused by robot tilting can be omitted for this application. Although this feature is not well documented, the GNSS is able to calculate both precise position and orientation even if the antennas are not in the same height.

Certain amount of data has to be transmitted from base-station to the data to achieve RTK solution. The data were transmitted through our custom micro-wave datalink that is able to transfer up to 1 Mbit/sec. The datalink was used for several other purposes, like remote control of the robot in manual mode, remote control of the auto-mode system parameters and inspection, during the experiment. The necessary communication reach was about 200 meters in our case, what was well suited for our datalink. If necessary the communication datalink may be substituted by other technologies, since the physical connection coming from our robot may vary from Ethernet, to CAN or RS 232/485. So the communication with the robot may be easily extended.

3 Path Planning and Navigation

Path-planning and navigation algorithms for autonomous robot navigation are described in the two following sections.

3.1 Waypoint Calculation

The complete path planning algorithm may be described as follows (see Figure 5).

1. Four points A, B, C, D surrounding the area of interest have to be defined manually.
2. The area is divided into defined number of sections in two axis defined by points AB, AC.
3. Numbered array of waypoints is calculated.

When the numbered waypoint network is defined, the robot can traverse them in corresponding order.

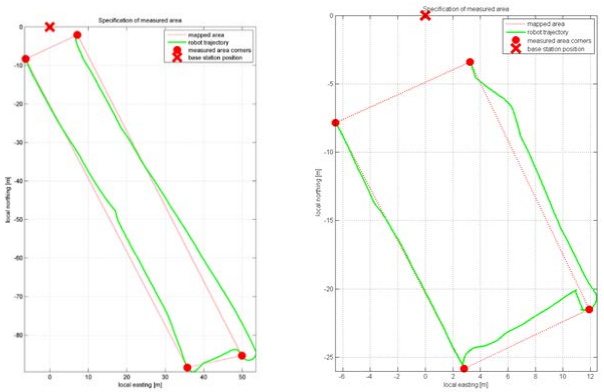

Fig. 5 Area of interest definition – demonstrated on data from the second experiment.

3.2 Navigation

Calculation using rhumb line is used for recalculation the measured GNSS main antenna position coordinates to the point lying in the robot rotation axis.

$$\varphi_c = \varphi_m - \frac{l_a}{R}\cos\theta\,, \tag{1}$$

$$\lambda_c = \lambda_m - \left(\ln\left(\tan\left(\frac{\varphi_m}{2}+\frac{\pi}{4}\right)\right) - \ln\left(\tan\left(\frac{\varphi_c}{2}+\frac{\pi}{4}\right)\right)\right)\tan\theta, \tag{2}$$

where φ_c, φ_m – latitude recalculated, measured, l_a – distance between antenna and rotation axis in horizontal plane, R – substitute sphere radius, λ_c, λ_m – longitude recalculated, measured, θ – mobile robot azimuth.

The whole trajectory control scheme may be described using **Chyba! Nenalezen zdroj odkazů.**. Rhumb line computing – makes rhumb line parameters calculation (azimuth θ_d and length d), both the initial robot center point (φ_c, λ_c) and the endpoint (waypoint φ_w, λ_w) are known.

$$\theta_d = \arctan\frac{\lambda_w - \lambda_c}{\ln\left(\mathrm{tg}\left(\frac{\varphi_w}{2}+\frac{\pi}{4}\right)\right) - \ln\left(\mathrm{tg}\left(\frac{\varphi_c}{2}+\frac{\pi}{4}\right)\right)}, \tag{3}$$

$$d = R\frac{\varphi_w - \varphi_c}{\cos\varphi_w} \tag{4}$$

The azimuth error is calculated as the difference between the requested azimuth of robot (rhumb line azimuth) and the actual robot azimuth – as measured between the RTK GNSS onboard antennas.

P controller with saturation is used for azimuth speed control. Saturation point is set to max. 50°. The maximum rotation speed is set as approximately 50% of the maximum forward speed.

ISBN: 978-1-61804-356-6

Forward robot speed is limited depending on azimuth regulation deviation. Forward speed is blocked approximately on deviation out of -50° to +50° range. If the deviation is 0°, the speed is not limited, so the transmission is 1.

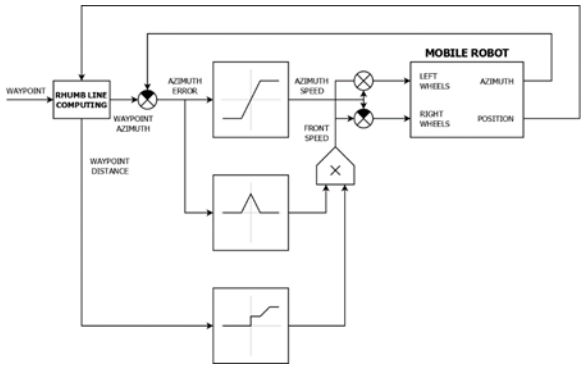

Fig. 6 Trajectory control scheme.

Forward speed limitation is also used when robot approaches a waypoint (distance < 10 cm). Here the maximum speed is limited down to 20 % of maximum forward speed. The limitation also depends on requested waypoint approach precision.
The speed of left (right) wheels is calculated as sum (difference) of forward and rotation robot speed. Robot center position calculation is based on position antenna measurement. Robot azimuth calculation is based on vector and position onboard antennas measurement.

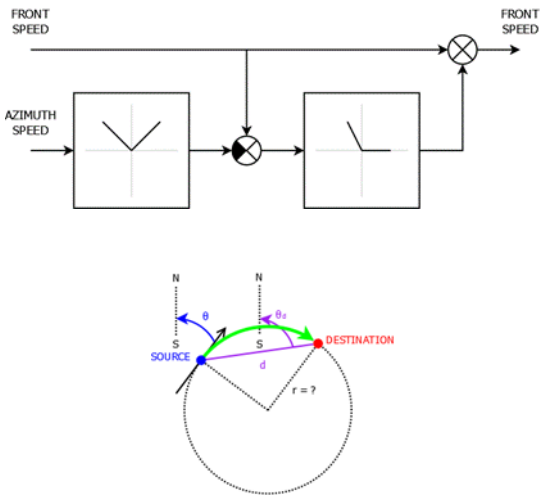

Fig. 7 Momentum reduction scheme (up), trajectory circle radius calculation (down).

Since differential drive configuration is used on Orpheus-X3 robot, the steering is done by skidding. That means extreme values of momentum forces applied on wheel/gearbox shafts. To avoid potential mechanical or electronics damage, we introduced minimum rotation radius, by which the wheels on both sides of the robot still rotate with the same direction. Slower wheel speed value is chosen as 20% of rotation speed (see Figure 7 left).

By introducing a minimal rotation radius, it may happen that several waypoints become unreachable. The unreachable point does not meet the following condition:

$$r < \left|\frac{d}{2\sin(\theta_d - \theta)}\right|, \tag{5}$$

where r is the defined minimum rotation radius, d is actual robot-to-waypoint, θ_d is rhumb line azimuth, θ is mobile robot azimuth (see **Chyba! Nenalezen zdroj odkazů.** down).

4 Experiments

Two practical experiment were done with the described equipment. The experiments were done as cooperation between SURO v.v.i. and Brno University of Technology.

4.1 Ground radioactive contamination measurement experiment

The aim of the first experiment was to measure radiation caused by La-140 isotope dust spread on grass-covered meadow.
In this experiment the robot was controlled remotely by operator in real-time, so the autonomous movement was not used. RTK GNSS technique was only used for precise position data-logging.
The results of the experiment are positive – it proved the use of Orpheus robotic system for remote radiation measurement is possible and profitable.
The experiment also proved it would be extremely profitable to have fully autonomous robot movement during the experiment – both for higher precision of the path and to be more considerate to the mechanical parts of the robot.

4.2 Lost radiation sources experiment

The second experiment was somewhat different. The main idea was to localize randomly located sealed radiation sources.

ISBN: 978-1-61804-356-6

The main difference from technical point of view was use of the fully autonomous path-planning and navigation, as described in Chapter 3.
Two measurements were done – one on greater area and one on smaller (see Figure 5) to be able to test influence of more dense data on explanatory value of the experiment.

Table 3. Large area surrounding polygon (see **Chyba! Nenalezen zdroj odkazů.**)

Pt1	Pt2	distance[m]	division	span[m]
A	D	14.8	15	0.99
B	C	14.52	15	0.97
A	B	90.48	18	5.03
C	D	93.61	18	5.20

Table 4. Small area surrounding polygon (see **Chyba! Nenalezen zdroj odkazů.**)

Pt1	Pt2	distance[m]	division	span[m]
A	D	10.74	10	1.07
B	C	10.07	10	1.07
A	B	20.28	20	1.01
C	D	20.07	20	1.00

The measurement was performed on grass-covered meadow nearby Trebic, Czech Republic. The area of interest (points A, B, C, D – see Figure 5) was marked by the robot controlled manually, the division to appropriate parts was done automatically by hereinbefore described algorithms to form approximately 1 m x 5 m rectangles in the first case (see Table 3) and approximately 1 m x 1 m in the second case (see Table 4).
The resulting network with automatically generated waypoints is on Figure 8 upper left and right, and Figure 9 upper left and right. The resulting intensity map is on Figure 8 lower, and Figure 9 lower.

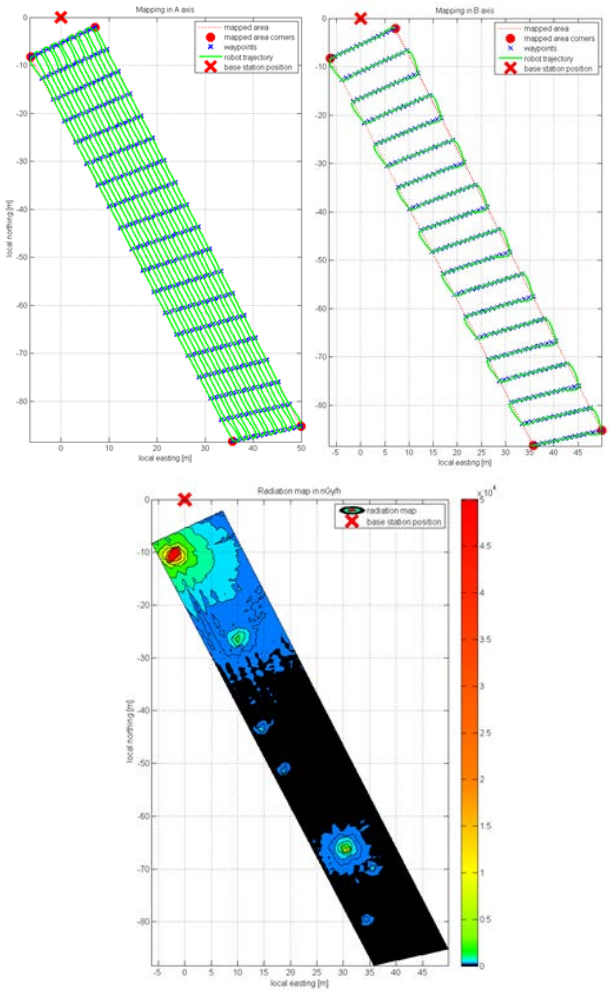

Fig. 8 Results - large area; horizontal (upper left), and vertical (upper right) span with waypoints and real traversed trajectory, resulting intensity map (lower).

ISBN: 978-1-61804-356-6

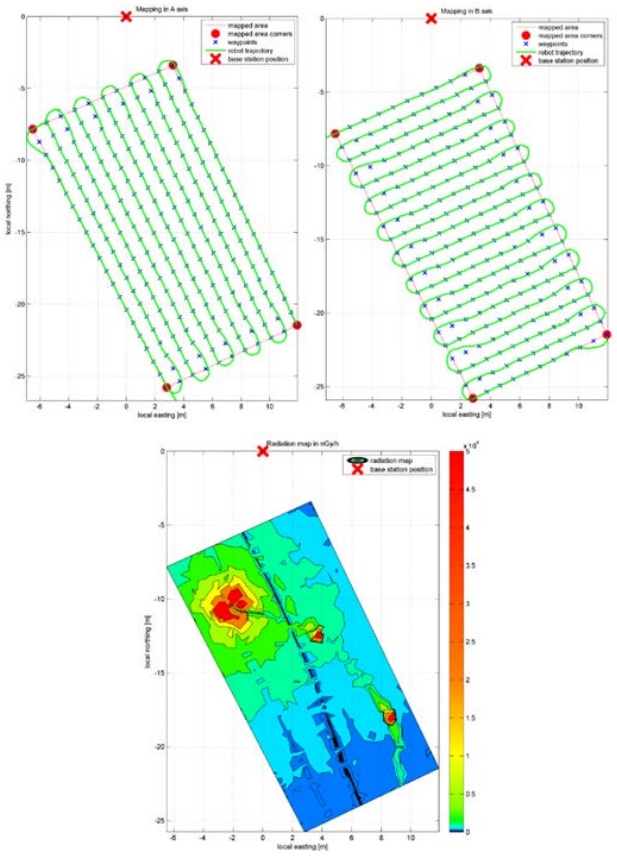

Figure 9. Results - small area; horizontal (upper left), and vertical (upper right) span with waypoints and real traversed trajectory, resulting intensity map (lower).

6 Conclusion

As it is visible on the results Figure 8 right, and Figure 9 right, the measurements were successful. It is obvious the autonomous path-planning, waypoint generation and navigation using precise RTK GNSS helped a lot to acquire consistent data. It also minimizes potential risk of operator error causing the measurement might be completely useless due to small part not being traversed and measured.

The same RTK GNSS complete was used for two different tasks in the second experiment – precise time and position data logging and robot navigation.

The original idea provided by the customer was to use classical GPS that is onboard the scintillation radiation sensor. Instead we proposed and designed system that relies on RTK GNSS with substantially higher precision. The result may be easily compared from Figure 9 lower and Figure 10 up. The later graph demonstrates the same measurement bused on data from the named low-resolution non-RTK GPS.

The advantage of fully autonomous robotic exploration and measurement in areas contaminated by radiation is obvious.

The resulting gamma-radiation diagram aligned with aerial photo is on Figure 10 down.

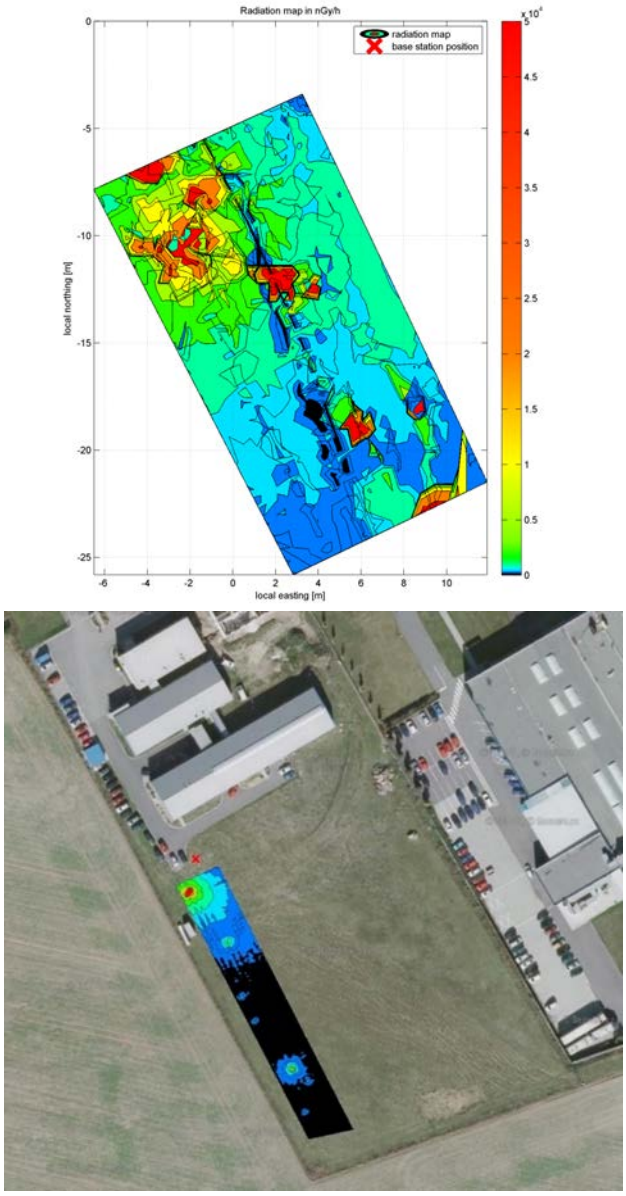

Figure 10. Resulting gamma-radiation diagram in aerial photo (up); demonstration of intensity diagram calculated based on imprecise data from non-RTK GNSS (down).

The hereinbefore described approach can be used for many environmental-related tasks. Autonomous robot can “quard” pre-defined area, e.g. around nuclear power-plant, for contamination. Contrary to people the robot will never be exhausted, even if it is hit by high amount of radiation, it will more likely sustain it and even if not, its value is definitely lower than the one of human beings. Furthermore the robot can do many other tasks in the area – e.g. guard against hostiles, make thermal images to prevent fire and/or technological issues, etc.

ISBN: 978-1-61804-356-6

Acknowledgments

This work was supported by VG 2012 2015 096 grant named Cooperative Robotic Exploration of Dangerous Areas by Ministry of Interior, Czech Republic, program BV II/2-VS.

This work was supported by the project CEITEC - Central European Institute of Technology (CZ.1.05/1.1.00/02.0068) from the European Regional Development Fund and by the Technology Agency of the Czech Republic under the project TH01020862 "System for automatic/automated detection/monitoring radiation situation and localisation of hot spots based on a smart multifunctional detection head usable for stationary and mobile platforms incl. unmanned".

References:

[1] http://www.dpie.com/datasheets/gps/Trimble-BX982-Datasheet-Document-581007.pdf, 12.12.2014, TRIMBLE BX982 datasheet

[2] http://www.leica-geosystems.be/downloads123/zz/airborne/fpes/brochures/Leica_FPES_BRO.pdf15.12.2014, Leica FPES Flight Planning & Evaluation Software

[3] T. M. Driscoll, Complete coverage path planning in an agricultural environment, Iowa State University, Graduate Thesis, 2011, 5.12.2014, http://lib.dr.iastate.edu/cgi/viewcontent.cgi?article=3053&context=etd

[4] I. A. Hameed, Intelligent Coverage Path Planning for Agricultural Robots and Autonomous Machines on Three-Dimensional Terrain, Journal of Intelligent Robot Systems, Springer, 2012

[5] S.W. Moon, D. H. Shim, Study on Path Planning Algorithms for Unmanned Agricultural Helicopters in Complex Environment, International Journal of Aeronautical and Space Science, 2009, vol. 10. No. 2.

[6] H. Eisenbeiss, APPLICATIONS OF PHOTOGRAMMETRIC PROCESSING USING AN AUTONOMOUS MODEL HELICOPTER, symposium ISPRS Commission Technique I "Des capteurs a l'Imagerie", n°185, 2007

[7] L. Zalud, F. Burian, L. Kopecny, and P. Kocmanova, ”Remote Robotic Exploration of Contaminated and Dangerous Areas”, in *International Conference on Military Technologies*, pp 525-532, Brno, Czech Republic, ISBN 978-80-7231-917-6, 2013.

[8] L. Zalud and P. Kocmanova, “Fusion of thermal imaging and CCD camera-based data for stereovision visual telepresence”, in *2013 IEEE International Symposium on Safety, Security, and Rescue Robotics* (SSRR). Linkoping: IEEE, 2013, pp. 1-6. DOI: 10.1109/SSRR.2013.6719344. ISBN 978-1-4799-0880-6

[9] P. Kocmanova, A. Chromy, L. Zalud, “3D Proximity Laser Scanner Calibration”, in 2013 18TH INTERNATIONAL CONFERENCE ON METHODS AND MODELS IN AUTOMATION AND ROBOTICS (MMAR), pp 742-747, ISBN 978-1-4673-5508-7

[10] L. Nejdl, J. Kudr, K. Cihalova, et. al. “Remote-controlled robotic platform ORPHEUS as a new tool for detection of bacteria in the environment”, in ELECTROPHORESIS, Volume: 35 Issue: 16 , Special Issue: SI, Pages: 2333-2345, 10.1002/elps.201300576

[11] L. Zalud, L. Kopecny, F. Burian, “Robotic Systems for Special Reconnaissance”, International Conference on Military Technologies, pp 531-540, Brno, Czech Republic, ISBN 978-80-7231-649-6, Oprox, 2009